Heliyon 10 (2024) e28077

Contents lists available at ScienceDirect

Heliyon

journal homepage: www.cell.com/heliyon

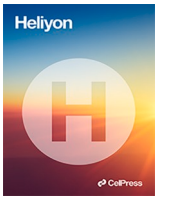

Research article

Shade responses and resistant mechanisms in *Spatholobus suberectus*

Shuangshuang Qin [a], Ying Liang [a], Guili Wei [a], Fan Wei [a], Kunhua Wei [a], Xiaoying Chen [a,*]

[a] *Guangxi Key Laboratory of Medicinal Resources Protection and Genetic Improvement/Guangxi Engineering Research Center of TCM Resource Intelligent Creation, National Center for TCM Inheritance and Innovation, Guangxi Botanical Garden of Medicinal Plants, Nanning 530023, China*

ARTICLE INFO

Keywords:
Spatholobus suberectus dunn
Shade treatment
Flavonoids
Transcriptomic gene expression
Cis-regulatory element

ABSTRACT

The medicinal plant *Spatholobus suberectus* Dunn is easily exposed to shade stress during growth, but its shade responses and shade stress resistant mechanisms have not been clarified. In this study, shade treatments including four attenuated sunlight intensities (100%, 60%, 40%, and 10%) and three shade durations (30 d, 45 d, and 60 d) were applied to *S. suberectus*. The shade-induced morphological indicators, phytohormonal regulations, metabolic flavonoids contents, transcriptomic flavonoid pathway gene expressions, and stress physiological changes of *S. suberectus* were analyzed. The putative promoter *cis*-regulatory elements (CREs) of 18 flavonoid biosynthetic pathway genes were identified. Results showed the stem growth indicators of *S. suberectus* were better at 40% light intensity. Phytohormones were involved in the shade-induced responses. Short-term shade (30 d) increased total flavonoids, gallated catechins and especially epigallocatechin gallate contents and favored for boosting medicinal value. Long-term shade (45 d, 60 d) tended to decrease flavonoids. The shade-induced flavonoids changes were attributed to their corresponding biosynthesizing genes expression variations. The high antioxidant capacity and the presence of phytohormone-, stress-, and development-related CREs provided the basis for stress resistance. In conclusion, the multiple responses under shade and the CREs analysis elucidated *S. suberectus*' shade tolerance.

1. Introduction

Spatholobus suberectus Dunn is the only officially recognized authentic source of Chinese herbal medicine *Spatholobi caulis* (Chinese name *ji xue teng*) in China Pharmacopeia. It has various pharmaceutical effects and long been used in China since the 17th century [1, 2]. It is usually utilized for treating gynecological (menoxenia, amenorrhea, and dysmenorrhea) and cardiovascular diseases, later more pharmacological activities (anticancer, antioxidant, anti-inflammatory, antirheumatic, anti-diabetic, and neuroprotective) were discovered [3].

The extensive usages of *S. suberectus* are mainly attributed to its flavonoids, which are the key therapeutic components in *S. suberectus*. In our former studies, we collected eight-year-old cultivated *S. suberectus* and quantified total flavonoids in all the five tissues, showing that the highest percentage of flavonoids were in the stem (Stem, ~2.3%; flower, ~1.3%; root, ~1.2%; fruit, ~0.7%;

* **Corresponding author**.
E-mail addresses: qin_double@126.com (S. Qin), 198yingzi@163.com (Y. Liang), weigl1992@163.com (G. Wei), fanwei_gx@163.com (F. Wei), divinekh@163.com (K. Wei), chxying2018@126.com (X. Chen).

https://doi.org/10.1016/j.heliyon.2024.e28077
Received 16 November 2023; Received in revised form 7 March 2024; Accepted 11 March 2024
Available online 12 March 2024

and leaf, ~0.7%), and that catechins were the most abundant flavonoids (~72.8%) in the stem (Catechins contents in other tissues were: Fruit, ~22.1%; root, ~7.4%; leaf, ~3.9%; and flower, ~0.5%). This result explained why stems were the traditionally used medicinal parts of *S. suberectus* [4]. We also detected eight forms of catechins in *S. suberetus*, including four non-gallated catechins (catechin, epicatechin, gallocatechin, and epigallocatechin) and their gallated forms (catechin gallate, epicatechin gallate, gallocatechin gallate, and epigallocatechin gallate). In addition, we detected another important natural flavonoid—isoliquiritigenin in *S. suberectus*. But isoliquiritgenin contents were comparatively low in stem while higher in root and flower (Isoliquiritigenin contents: Root > flower > fruit > stem > leaf) [4].

In our other previous studies, we assembled a chromosome scale genome (798 Mb) of *S. suberectus* (2n = 18), functionally annotated 31 634 (93.9%) protein-coding genes [5]. This genomic dissection combined with RNA sequencing (RNA-seq) data helped us to identify 163 genes involving in flavonoid biosynthesis and picture an elaborate flavonoid biosynthetic pathway in *S. suberectus* as follows [4] (Fig. 1): In the general phenylpropanoid pathway, phenylalanine is catalyzed by phenylalanine ammonialyase (PAL), cinnamate-4-hydroxylase (C4H), and 4-coumaroyl-CoA ligase (4CL) to form 4-coumaroyl-CoA, which is the branch point for flavonoid biosynthesis pathway. Chalcone synthase (CHS) is the first enzyme entering into flavonoid pathway, condensing one molecule of 4-coumaroyl-CoA and three molecules of malonyl-CoA to form naringenin chalcone. Naringenin chalcone can be catalyzed by chalcone reductase (CHR) to form isoliquiritigenin, or be catalyzed by chalcone isomerase (CHI) to form naringenin. Naringenin is the central point for various flavonoids (flavones, isoflavones, flavonols, flavanols, anthocyanins, and proanthocyanidins). In the flavanols (catechins) branch pathway, naringenin generates dihydrokaempferol under the catalysis of flavanone 3-hydroxylase (F3H), and dihydrokaempferol can be converted to dihydroquercetin by flavonoid 3′-hydroxylase (F3′H). The next step is dihydroflavonols (dihydrokaempferol and dihydroquercetin) converting to leucoanthocyanidins by dihydroflavonol-4-reductase (DFR). Then leucoanthocyanidins can be catalyzed by leucoanthocyanidin reductase (LAR) to form catechin/gallocatechin, or be catalyzed by anthocyanidin synthase (ANS) and anthocyanidin reductase (ANR) to form epicatechin/epigallocatechin. And these non-gallated catechins can be converted to their gallated forms (catechin gallate, gallocatechin gallate, epicatechin gallate, and epigallocatechin gallate). Altogether, we identified 18 genes in this flavonoid biosynthetic pathway of *S. suberectus*, namely *SsPAL1, SsPAL2, SsC4H1, SsC4H2, Ss4CL1, Ss4CL2, SsCHS, SsCHR, SsCHI, SsF3H, SsF3′H, SsDFR1, SsDFR2, SsLAR1, SsLAR2, SsANS, SsANR1,* and *SsANR2*.

The putative promoter *cis*-regulatory elements (CREs) analyses of the aforementioned 18 flavonoid biosynthetic pathway genes could give information about interested CREs, such as phytohormone-, stress-, and development-related CREs in *S. suberectus*. Plant CREs mediate gene expression regulations at transcriptional and post-transcriptional level and the CREs' copy number, position/location, orientation affect their function [6,7]. Analysis of CREs helps to dissect genes functions and facilitates to understand how genes resist different kinds of stresses.

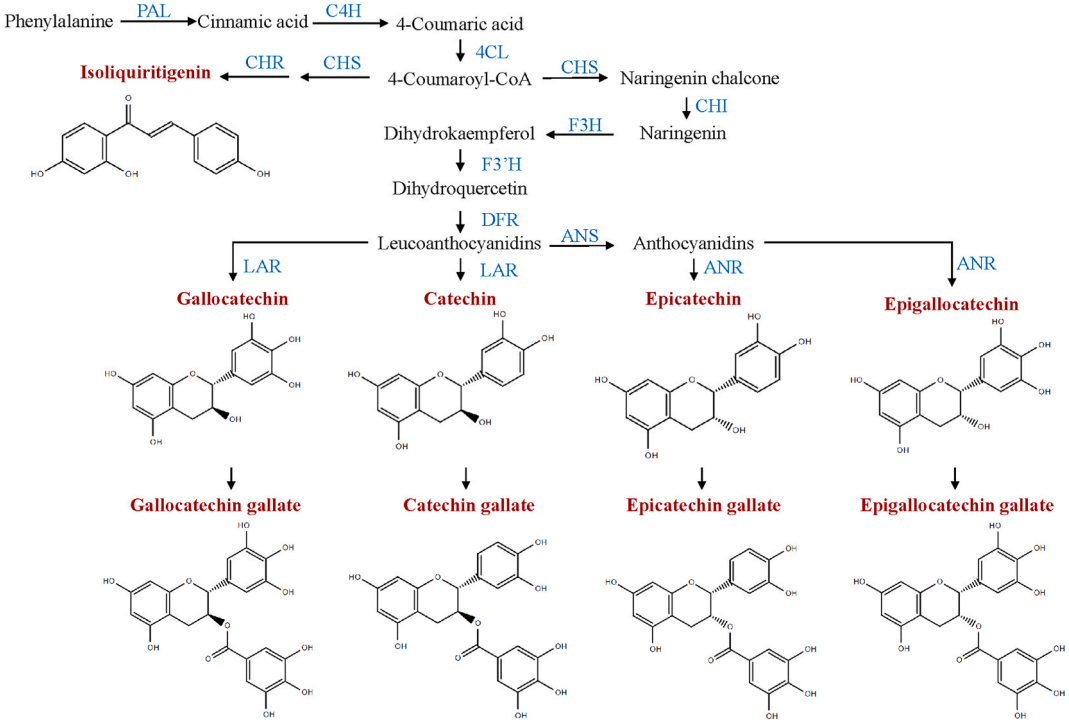

Fig. 1. The major flavonoids biosynthetic pathway in *Spatholobus suberectus*.
Abbreviations: PAL, phenylalanine ammonialyase; C4H, cinnamate-4-hydroxylase; 4CL, 4-coumaroyl-CoA ligase; CHS, chalcone synthase; CHR, chalcone reductase; CHI, chalcone isomerase; F3H, flavanone 3-hydroxylase; F3′H, flavonoid 3′-hydroxylase; DFR, dihydroflavonol-4-reductase; LAR, leucoanthocyanidin reductase; ANS, anthocyanidin synthase; ANR, anthocyanidin reductase.

S. suberectus is a subtropical perennial woody climber or scandent shrub or subshrub. Wild *S. suberectus* grows in open or dense forests, scrubs, valleys and mountain slopes at high altitude (800–1700 m). The climbing plant characteristics and the wide range of living habitats of *S. suberectus* make it more flexible to light environmental changes, especially shade. Yet no experimental proofs have been provided to justify whether *S. suberectus* is shade-tolerant or not. What decides the shade responses of *S. suberectus*? Whether shade is beneficial or unfavorable for boosting the medicinal value of *S. suberectus* is still unknown. If shade improves the medicinal value of *S. suberectus* as wishes, just like some other reported medicinal herbs [8–12]? What is the underlying shade tolerant mechanism of *S. suberectus*? All these questions need to be clarified and systematically discussed.

Nowadays, wild *S. suberectus* is vulnerable because of overharvesting and its low natural seed reproductive capacity. To answer the above-mentioned questions of this study, successful cultivation system of *S. suberectus* needs to be constructed first. Our cultivation work had avoided this low reproductive defect by cutting seedlings, and the survival rate of two-year-old *S. suberectus* could reach 85% or much higher. Moreover, the demonstration of stem cross sections from our cultivated eight-year-old *S. suberectus* exhibited similar anatomical feature to wild *S. suberectus*, which had concentric/eccentric ring arranged alternatively by xylem and red-brown phloem layers [13] (Fig. 2A–F). This further proved our planting techniques were efficient.

The aim of this study was to uncover the shade-induced multiple responses and explore the shade resistant mechanisms in *S. suberectus*. Shade treatments including four attenuated sunlight intensities (100%, 60%, 40%, and 10%) and three shade durations (30 d, 45 d, and 60 d) were applied to two-year-old cultivated *S. suberectus*. The morphological indicators, phytohormonal regulations, metabolic flavonoids contents, transcriptomic flavonoid pathway gene expressions, and stress physiological changes of *S. suberectus* under shade treatments were analyzed. The phytohormone-, stress-, and development-related CREs of flavonoid biosynthetic pathway genes were identified. Collectively, we offered evidences for *S. suberectus*' shade tolerance and illustrated the related mechanisms. We demonstrated that short-term shading (30 d) improved medicinal value in *S. suberectus*. Our work is useful for the planting, management and boosting profits of *S. suberectus*.

2. Materials and methods

2.1. Plant material, shade treatment, and sampling

Spatholobus suberectus Dunn was cultivated in Guangxi Botanical Garden of Medicinal Plants , Nanning, China (22°51′28″ N, 108°22′2″ E). This region is a low-latitude subtropical monsoon climate zone in Southern China, with an annual mean temperature of 21.6 °C and an annual mean precipitation of 1304.2 mm.

In February 2019, stem cuttings of *S. suberectus* (1 cm in diameter, with three nodes) were planted in the experimental field. The cultivation area was 240 m^2 (12 × 20). The row spacing was 0.6 m × 0.6 m. The cuttage rooting rate was 92.2%. In May 2020, shade treatments were performed on *S. suberectus*. Light intensities were recorded at 9:30–10:00 a.m. on a sunny day by UPRtek MK350 N PLUS spectrometer (Zhunan Township, Miaoli County, Taiwan). The field natural sunlight was used as control (100%, ~53760 lux). The other three attenuated light gradients obtained by covering black shade nets were 60% (~33857 lux), 40% (~20400 lux), and 10% (~4675 lux). The shade treatments were continued for 30 days, 45 days, and 60 days, respectively. And 30 plants were assigned to each shade treatment. Open all-around shade was applied to improve air circulation and keep consistent temperature among shade treatments. In brief, the shade treatments included four attenuated sunlight intensities (100%, 60%, 40%, and 10%) and three shade

Fig. 2. *Spatholobus suberectus* images. Wild (A), two-year-old- (B) and eight-year-old- (C) cultivated *S. suberectus* and their respective stem cross-sections (D, E, and F).

durations (30 d, 45 d, and 60 d).

For the following determination of phytohormone contents, metabolic flavonoids contents, transcriptomic gene expressions, and stress physiological parameters, samplings were taken from the 30 d-, 45 d-, and 60 d-shade-treated fresh stems of *S. suberectus*. Each sampling included three biological replicates. All the taken samples were put into liquid nitrogen for 30 min and then stored at −80 °C. To prevent sample RNA degradation and other unexpected damages, all experimental items were done as soon as possible.

2.2. Plant growth morphological parameter measurement

The four growth morphological parameters of *S. suberectus*, including basal stem diameter increment, new stem diameter increment, new stem height increment, and leaf number increment, were measured at the three sampling times (30 d, 45 d, and 60 d).

2.3. Phytohormone content determination

Four plant hormone contents were determined. Briefly, 1.0 g samples were dissolved in 5 mL phosphate buffer solution (PBS, 0.01 M, pH7.4) and grinded into homogenate. After centrifuged at 2500 rpm for 20 min, the supernatants were collected and stored at −20 °C. Plant auxin (IAA) kit (MLBIO, ml147100, China), plant gibberellin (GA) kit (MLBIO, ml077232, China), plant methyl jasmonate (MeJA) kit (MLBIO, ml036358, China), and plant abscisic acid (ABA) kit (MLBIO, ml062458, China) were used for the phytohormone content determination.

2.4. Total flavonoids, catechins, and isoliquiritigenin content determination

The extraction of total flavonoids in *S. suberectus* was as follows: Weighted 0.3 g freeze-dried stem powder samples, dissolved in 25 mL 50% ethanol, and ultrasonic extracted for 1 h (SB-800 DTD ultrasound, Ningbo Xinzhi Biotechnology Co., Ltd.; power: 100 W; frequency: 40 kHz). Total flavonoids content was assessed spectrophotometrically by using rutin (National institute for control of pharmaceutical and biological products, Beijing, China) as a reference standard. The reactions of rutin with chromogenic reagent ($NaNO_2$–$Al(NO_3)_3$–NaOH) could produce reddish-orange product and be observed by absorbance. Followed was the detailed procedure: The rutin solutions (0.5 mg/mL, dissolved in 50% ethanol) were pipetted serially (0.5, 1.0, 1.5, 2.0, 2.5, and 3.0 mL) into a 25 mL volumetric flask, added 1 mL 5% $NaNO_2$ and incubated for 5 min, then added 1 mL 10% $Al(NO_3)_3$ and incubated for another 5 min, afterwards added 10 mL 4% NaOH and diluted with 50% ethanol to final volume, after incubated for 10 min, the absorbance was measured at 505 nm with an ultraviolet–visible spectrophotometer (Varian, United States). The standard curve of rutin was plotted eventually. Total flavonoids content of *S. suberectus* was calculated as rutin equivalent.

Catechins and isoliquiritigenin, the major flavonoids in the stem of *S. suberectus*, were quantified by ultra-performance liquid chromatography tandem triple quadrupole mass spectrometry (UPLC-QQQ-MS/MS). Prior to the analysis, 0.02 g freeze-dried stem powder samples were extracted with 1.5 mL 70% methanol at 50 °C for 2 h, centrifuged at 12 000 rpm for 10 min at room temperature, cooled the supernatant and added pure methanol up to 1.5 mL, centrifuged again and filtrated supernatants through 0.22 μm syringe filters (PALL, Ann arbor, MI, United States). Next, the extractions were eluted by ACQUITY® UPLC I-Class system (Waters, Milford, MA, United States). The chromatographic column was Acquity UPLC BEH C18 column (100 mm × 2.1 mm, 1.8 μm) (Waters). The mobile solvent A was ultrapure water containing 0.1% formic acid and the mobile solvent B was acetonitrile containing 0.1% formic acid. The column temperature was 40 °C. The injection volume was 1.0 μL. The flow rate was 0.6 mL/min. The gradient elution procedure was as follows: 0–1.0 min, 95% (v/v) A; 1.0–3.5 min, 95-70% (v/v) A; and 3.5–5.5 min, 70-40% (v/v) A. Followed the chromatographic analysis was the coupled electrospray ionization (ESI, negative ion) QQQ-MS/MS detection using QTRAP® 6500 system (AB SCIEX, Los Angeles, CA, United States) in the multiple reaction monitoring (MRM) mode. The optimal mass spectrometry operation settings were ion spray voltage, 4500 V; curtain gas (nitrogen), 35 psi; and turbo gas temperature, 550 °C. The optimized chromatographic retention time (min), precursor-product ion pairs of *m/z*, declustering potential (DP), collision energy (CE), and cell exit potential (CXP) specific for eight catechins (catechin, epicatechin, gallocatechin, epigallocatechin, catechin gallate, epicatechin gallate, gallocatechin gallate, and epigallocatechin gallate) and isoliquiritigenin were shown in Table 1. The details of their reference standards, that is, Lot number, purity (98% or higher), and manufacturer (Beijing Solarbio Science & Technology Co., Ltd, Beijing,

Table 1
Mass spectrometry parameters for quantification of catechins and isoliquiritigenin.

Compounds	Chromatographic retention time (min)	Precursor-product ion pairs of *m/z*	DP/V	CE/V	CXP/V
Catechin	1.83	288.9/202.9	−80	−27	−10
Epicatechin	2.53	289.1/203.0	−125	−27	−11
Gallocatechin	1.00	304.0/124.9	−175	−32	−15
Epigallocatechin	1.58	304.8/124.8	−147	−34	−25
Catechin gallate	3.89	441.1/168.9	−197	−25	−13
Epicatechin gallate	3.81	441.0/289.0	−150	−27	−11
Gallocatechin gallate	2.82	457.1/169.0	−118	−20	−23
Epigallocatechin gallate	2.57	457.0/169.1	−194	−24	−8
Isoliquiritigenin	1.48	463.1/300.0	−191	−36	−22

**m/z*, mass to charge ratio; DP, declustering potential; CE, collision energy; CXP, cell exit potential; V, voltage.

China) were listed in Supplementary table S1. The chromatograms of each reference standard were presented in Sup plementary fig. S1.

2.5. Transcriptomic gene expression in S. suberectus

For RNA-seq, a RNA library was constructed using NEBNext® Ultra™ II Directional RNA Library Prep Kit for Illumina® (NEB #E7760) and sequenced on an Illumina HiSeq™ 2000 platform. Transcriptomic data were mapped to the *S. suberectus* reference genome to identify studied genes. Transcript quantifications were estimated with RSEM (RNA-Seq by Expectation Maximization) software package (http://deweylab.github.io/RSEM/) [14], and Transcripts Per Million reads (TPM) values were used to represent transcriptomic absolute gene expression levels of structural genes involved in flavonoid synthesis.

2.6. Plant stress physiological parameter determination

The shade-induced eight stress physiological parameters, including soluble sugar, soluble protein, hydrogen peroxide (H_2O_2), superoxide anion radical ($O_2^-\cdot$), peroxidase (POD), superoxide dismutase (SOD), catalase (CAT), and malonydialdehyde (MDA), were tested according to their commercial assay kits. The respective assay kits were listed as follows: Plant soluble sugar kit (MLBIO, ml670187, China), plant soluble protein kit (MLBIO, ml680403, China), plant H_2O_2 kit (Geruisi-bio, G0112W, China), plant $O_2^-\cdot$ kit (Geruisi-bio, G0116W, China), plant POD kit (MLBIO, ml60732, China), plant SOD kit (MLBIO, ml606325, China), plant CAT kit (MLBIO, ml202784, China), and plant MDA kit (MLBIO, ml505357, China).

2.7. Promoter cis-regulatory element analysis

Promoter *cis*-regulatory elements were searched by PlantCARE [15] and validated by NEW PLACE [16]. The ~ 2 kb promoter sequences upstream from ATG of 18 flavonoid biosynthetic pathway genes (*SsPAL1, SsPAL2, SsC4H1, SsC4H2, Ss4CL1, Ss4CL2, SsCHS, SsCHR, SsCHI, SsF3H, SsF3′H, SsDFR1, SsDFR2, SsLAR1, SsLAR2, SsANS, SsANR1,* and *SsANR2*) of *S. suberectus* were used for searching for phytohormone-, stress-, and development-related *cis*-regulatory elements.

The visualization of targeted *cis*-regulatory elements was done by Clustergrammer [17]. The drawn heatmaps' row- and column-variables were ranked by variances.

2.8. Statistical analysis

Data were analyzed using IBM® SPSS® Statistics 19 (IBM, New York, United States). The sample normality distribution and

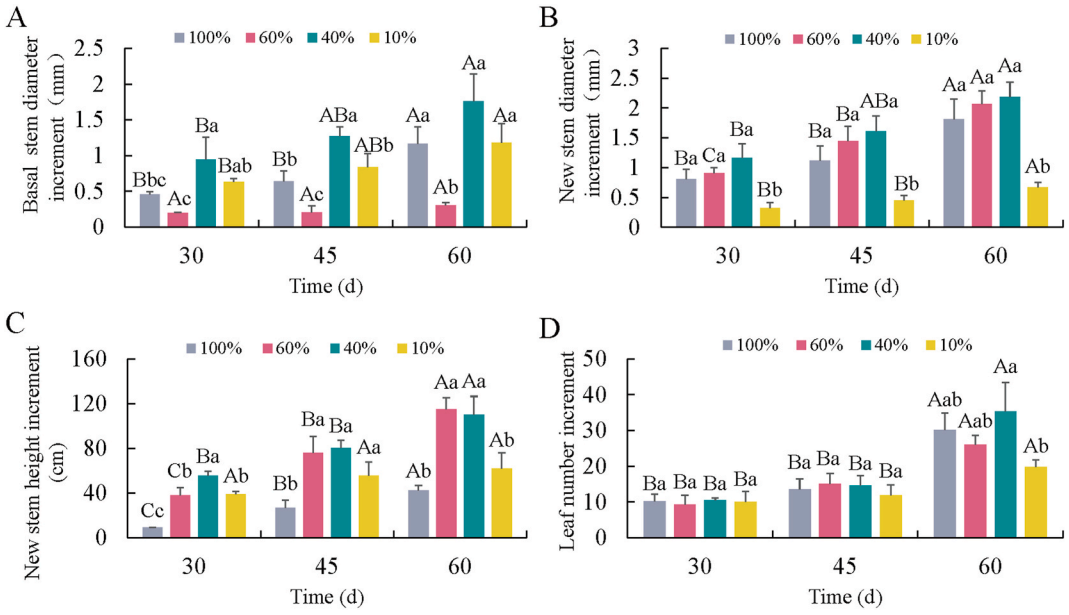

Fig. 3. Shade-induced morphological changes in *Spatholobus suberectus*. The shade treatments included four attenuated sunlight intensities (100%, 60%, 40%, and 10%) and three shade durations (30 d, 45 d, and 60 d). Lowercase and uppercase letters indicated statically significant differences respectively caused by light intensity ($p < 0.05$, a > b > c > d) and shade duration ($p < 0.05$, A > B > C > D). The bars indicate the means (±SD) of three independent replicates. (For interpretation of the references to colour in this figure legend, the reader is referred to the Web version of this article.)

homogeneity of variance between groups were tested. One-way analysis of variance (ANOVA) with post hoc (Duncan) tests assumed equal variances was performed to compare multiple groups' statistical significance. The probability (p) value set for determining statistical significance was $p < 0.05$ as statistically significant.

3. Results

3.1. Shade-induced morphological changes in S. suberectus

Four plant morphological indicators especially concerning the medicinal parts (stems) were recorded in the shade treatments. As shown in Fig. 3, when compared to the 100% light intensity control, the stem and leaf phenotypic parameters in the whole shade treatment durations exhibited different change patterns: (I) The basal stem diameter increments (Fig. 3A) were significantly decreased at 60% light intensity, while significantly or slightly increased at 40%- and 10%- light intensities. (II) The new stem diameter increments (Fig. 3B) were slightly increased at 60%- and 40%- light intensities, but significantly decreased at 10% light intensity. (III) The new stem height increments (Fig. 3C) were significantly or slightly increased at 60%-, 40%-, and 10%- light intensities, showing all shade treatments promoted stem elongations. (IV) The above three parameters were all increased and higher at 40% light intensity than (or at least comparable to) the other two intensities, indicating the 40% light intensity was more beneficial for the stem growth than 60%- and 10%- light intensities. (V) In contrast to the stems, leaf numbers were less affected and their increments (Fig. 3D) showed no significant differences in different light regimes. Overall, the stems' growth and morphology were altered when *S. suberectus* confronted with the light environmental changes.

3.2. Shade-induced phytohormonal changes in S. suberectus

The plant hormone changes in the shade treatments were shown in Fig. 4. The light-induced phytohormone changes included two aspects. First, from the shade duration aspect, along with the progress of the 30 d-, 45 d- and 60 d-shade durations, contents of IAA (Fig. 4A), MeJA (Fig. 4C) and ABA (Fig. 4D) at the 100% light intensity control were in an increased trend, which were in consistent with the plant sustainable growth. Contents of MeJA (Fig. 4C) and ABA (Fig. 4D) in the three shade treatments followed this developmental increase pattern. But Contents of IAA (Fig. 4A) and GA (Fig. 4B) in the three shade treatments were almost remained constant or even decreased (GA: 10% light intensity at 45 d), indicating this increases were inhibited by low light stress. Second, from the light intensity aspect, the variations were listed as follows: (I) The IAA contents (Fig. 4A) in the three shade treatments were statistically increased or comparable to the 100% light intensity control. The IAA levels at the 60%-, and 10%- light intensities were not statistically different, but they were higher than those of the 40% light intensity. (II) The GA contents (Fig. 4B) in shade treatments were statistically increased or unchanged compared to the control light intensity. The GA contents were all highest at 40% light intensity in the shade treatments. The second higher and the lowest GA contents were at 60%-, and 10%- light intensities, respectively. (III) The MeJA contents (Fig. 4C) at 60%- and 40%- light intensities were first similar to the control (30 d, and 45 d) and then significantly decreased in

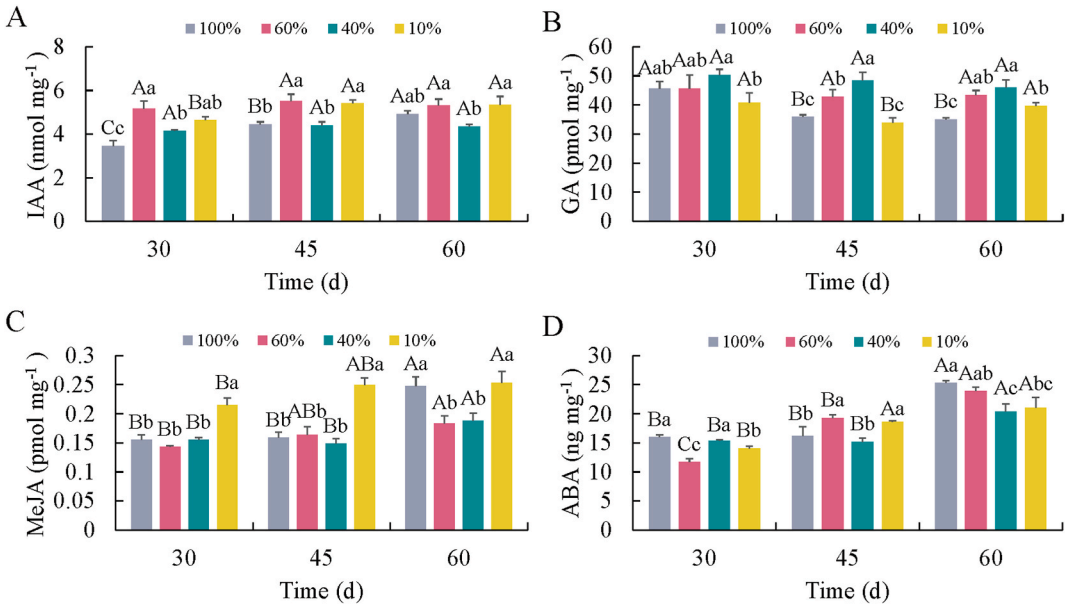

Fig. 4. Shade-induced phytohormonal changes in *Spatholobus suberectus*. IAA, auxin; GA, gibberellin; MeJA, methyl jasmonate; ABA, abscisic acid. Figure legends of shade treatments and statistical analyses are the same as in Fig. 3. (For interpretation of the references to colour in this figure legend, the reader is referred to the Web version of this article.)

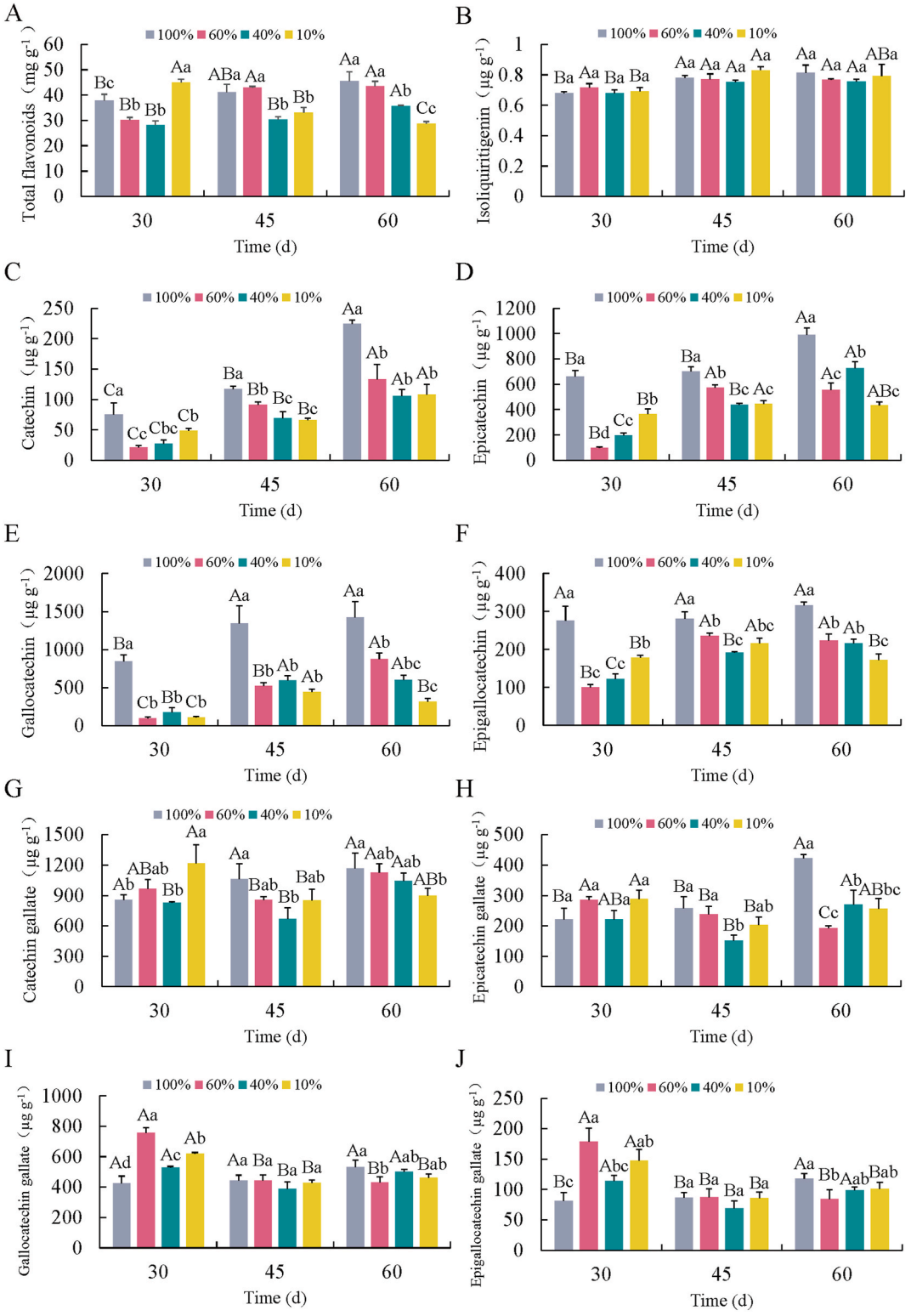

Fig. 5. Shade-induced flavonoid changes in *Spatholobus suberectus*. Figure legends of shade treatments and statistical analyses are the same as in Fig. 3. (For interpretation of the references to colour in this figure legend, the reader is referred to the Web version of this article.)

the end (60 d). The MeJA contents were highest at 10% light intensity during the whole shade treatments. (IV) The ABA contents (Fig. 4D) at 60%- and 40%- light intensities exhibited opposite change directions: The former were lower than other shading treatments at 30 d, but higher at 45 d and 60 d; the latter were higher at 30 d, but lower at 45 d and 60 d. The ABA content changes at 10% light intensity were between the 60%- and 40%- light intensities. In summary, IAA, GA, MeJA and ABA responded differentially to light

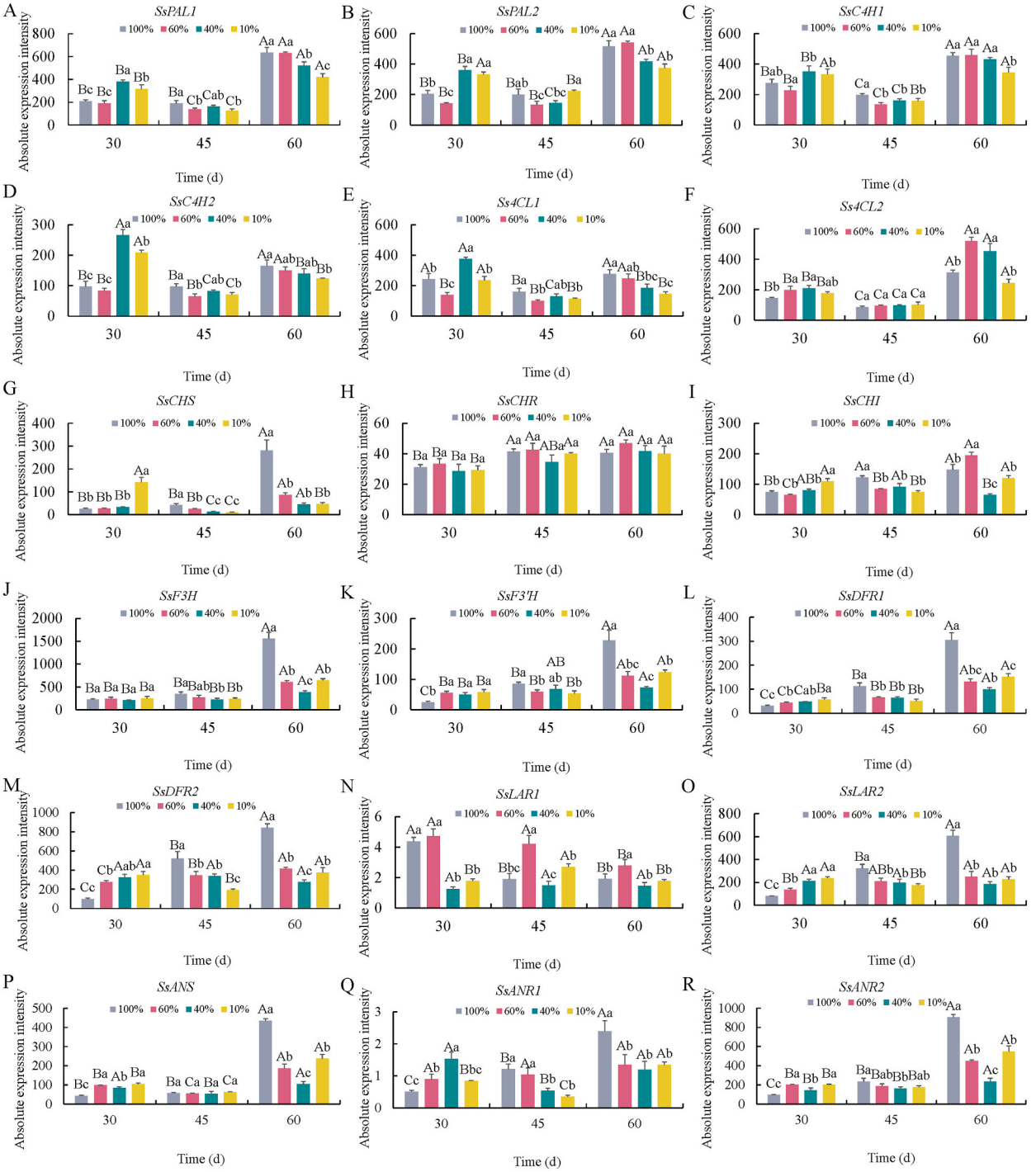

Fig. 6. Shade-induced flavonoid biosynthetic gene expression changes in *Spatholobus suberectus*. The transcriptomic absolute gene expression levels were represented by Transcripts Per Million reads (TPM) values. Abbreviations of enzymes are the same as in Fig. 1. Figure legends of shade treatments and statistical analyses are the same as in Fig. 3. (For interpretation of the references to colour in this figure legend, the reader is referred to the Web version of this article.)

environmental changes, implying their varied roles behind the shade treatments.

3.3. Shade-induced metabolic flavonoid changes in S. suberectus

The metabolic changes especially the pharmaceutical secondary metabolites (flavonoids) were demonstrated in Fig. 5. The metabolite variation regularities in the shade treatments were listed as follows: (I) Contents of isoliquiritigenin (Fig. 5B) were not affected either by light intensity or by shade duration. (II) Contents of total flavonoids (Fig. 5A), and eight forms of catechins (Fig. 5C–J) in the shade treatments were all significantly decreased or comparable to those of the control with increasing shade time (at 45 d- and 60 d-shade durations). (III) Short-term shading (30 d-shade durations) induced three change patterns: (i) Contents of total flavonoids (Fig. 5A) at 30 d-shade durations were significantly decreased at 60%- and 40%- light intensities but significantly increased at 10% light intensity. (ii) Contents of the four non-gallated catechins (catechin (Fig. 5C), epicatechin (Fig. 5D), gallocatechin (Fig. 5E) and epigallocatechin (Fig. 5F)) at 30 d-shade durations were significantly decreased compared to 100% light intensity control. (iii) Contents of the four gallated-catechins (catechin gallate (Fig. 5G), epicatechin gallate (Fig. 5H), gallocatechin gallate (Fig. 5I) and epigallocatechin gallate (Fig. 5J)) at 30 d-shade durations were significantly increased or comparable to those of the control. Catechin gallate (Fig. 5G) and epicatechin gallate (Fig. 5H) contents at 30 d-shade durations were all highest at 10% light intensity, but the latter were non-significant and barely changed among different light intensities. Epigallocatechin gallate (Fig. 5J), as the most potent (antioxidant/anticancer/anti-inflammatory) catechin, exhibited similar change patterns to its non-epistructured catechin (gallocatechin gallate) (Fig. 5I) in the whole shade treatments, and their contents at 30 d-shade durations were all highest at 60% light intensity. (IV) Time course analysis showed at 100% light intensity control, contents of metabolites (total flavonoids (Fig. 5A), and eight catechins (Fig. 5C–J)) were statistically increased (or unchanged) at 30 d-, 45 d- and 60 d-shade durations, which was in line with the plant developmental process. Similar time effects were seen at 60%- and 40%- light intensities (except for contents of epicatechin gallate (Fig. 5H), gallocatechin gallate (Fig. 5I), and epigallocatechin gallate (Fig. 5J)). On the contrary, at 10% light intensity, contents of some metabolites (total flavonoids (Fig. 5A), catechin gallate (Fig. 5G), epicatechin gallate (Fig. 5H), gallocatechin gallate (Fig. 5I), and epigallocatechin gallate (Fig. 5J)) followed a decrease pattern at 30 d-, 45 d- and 60 d-shade durations, indicating the normal 'flavonoid accumulated with plant development' pattern was interrupted by very low light intensity. Taken together, although exhibited ups or downs in short-term shading (30 d), flavonoid contents especially catechins tended to be down-regulated in long-term shading (45 d and 60 d).

3.4. Shade-induced transcriptomic flavonoid pathway gene expression changes in S. suberectus

Shade treatments resulted in key gene expression changes in *S. suberectus*. Gene expression levels of 18 flavonoid biosynthetic genes, namely *SsPAL1* (Fig. 6A), *SsPAL2* (Fig. 6B), *SsC4H1* (Fig. 6C), *SsC4H2* (Fig. 6D), *Ss4CL1* (Fig. 6E), *Ss4CL2* (Fig. 6F), *SsCHS* (Fig. 6G), *SsCHR* (Fig. 6H), *SsCHI* (Fig. 6I), *SsF3H* (Fig. 6J), *SsF3′H* (Fig. 6K), *SsDFR1* (Fig. 6L), *SsDFR2* (Fig. 6M), *SsLAR1* (Fig. 6N), *SsLAR2* (Fig. 6O), *SsANS* (Fig. 6P), *SsANR1* (Fig. 6Q), and *SsANR2* (Fig. 6R), were represented by RNA-seq data. The variation regularities were listed as follows: (I) Enzyme of CHR catalyzes the production of isoliquiritigenin. *SsCHR* expressions (Fig. 6H) were unaffected in all the shade treatments. Other 17 genes (Fig. 6A–G, Fig. 6I-R) responded to the light environmental changes. (II) The RNA-seq data of pathway gene expression levels at 60 d-were higher than those at 30 d- and 45 d-shade durations (except *SsC4H2* (Fig. 6D), *Ss4CL1* (Fig. 6E), and *SsLAR1* (Fig. 6N)), consisting with the sustained plant growth development. (IV) At 60 d-shade durations, except for *Ss4CL2* (Fig. 6F), *SsCHI* (Fig. 6I), and *SsLAR1* (Fig. 6N), whose gene expression levels were highest at 60% light intensity, the rest flavonoid biosynthetic genes expressions in the shade treatments were all decreased compared to the 100% light intensity control, implying the negative effects of long-term low light. (V) According to their functional specificity, the flavonoid biosynthetic gene expression variations could be classified into three types: (i) Enzymes of PAL, C4H, and 4CL catalyze phenylalanine to form 4-coumaroyl-CoA. At 30 d-shade durations, *SsPAL1* (Fig. 6A), *SsPAL2* (Fig. 6B), *SsC4H1* (Fig. 6C), *SsC4H2* (Fig. 6D), *Ss4CL1* (Fig. 6E) and *Ss4CL2* (Fig. 6F) expressions were highest at 40% light intensity. The first five genes expressions followed a decrease-increase-decrease pattern at 60%-, 40%-, and 10%- light intensities compared to control, while the last *Ss4CL2* gene expressions were increased at 60%- light intensity. At 45 d-shade durations, the six gene expression levels in shade treatments were decreased or equal to the control. At 60 d-shade durations, the first five genes expressions in shade treatments were gradually decreased as the light intensity lowered, while the last *Ss4CL2* gene expressions were significantly increased at 60%- and 40%- light intensities compared to control. (ii) Enzymes of CHS, and CHI catalyze 4-coumaroyl-CoA to form naringenin. At 30 d-shade durations, both *SsCHS* (Fig. 6G) and *SsCHI* (Fig. 6I) expressions were highest at 10% light intensity and unchanged at 60%- and 40%- light intensities. At 45 d-shade durations, the two expressions in shade treatments were significantly decreased compared to control. At 60 d-shade durations, *SsCHS* expressions in shade treatments were significantly decreased, while *SsCHI* expressions in shade treatments were increased at 60% light intensity. (iii) Enzymes of F3H and F3′H catalyze naringenin to form dihydrokaempferol or dihydroquercetin. Enzymes of DFR, ANS, ANR, and LAR catalyze dihydroflavonols to form catechins. *SsF3H* (Fig. 6J), *SsF3′H* (Fig. 6K), *SsDFR1* (Fig. 6L), *SsDFR2* (Fig. 6M), *SsLAR2* (Fig. 6O), *SsANS* (Fig. 6P), *SsANR1* (Fig. 6Q) and *SsANR2* (Fig. 6R) expressions in shade treatments were significantly increased or equal to control at 30 d-, significantly decreased or equal to control at 45 d-, and significantly decreased at 60 d-shade durations. Whereas the leftover *SsLAR1* expressions (Fig. 6N) were highest at 60%- and decreased or equal to control at 40%- and 10%- light intensities in all the three shade durations. Taken together, the functional genes expressions in shade treatments were mostly variated at 30 d-, narrowed the gap between shading and control at 45 d-, and decreased at 60 d-shade durations. These responses reflected the plant acclimation process to the low light stress.

3.5. Shade-induced stress physiological changes in S. suberectus

Physiological parameters related to abiotic resistance were demonstrated in Fig. 7. The adaptive stress response parameters included the following: (I) Soluble sugar and soluble protein not only provide nutrition and energy for plant growth but also act as osmoprotectants for plant stress resistance. The soluble sugar contents (Fig. 7A) of shade treatments were significantly or slightly increased compared to control except one case (60% light intensity at 30 d). And the soluble sugar contents were all highest at 10% light intensity compared to other light regimes and this trend continued as time prolonged. While no significant differences were observed in soluble protein contents (Fig. 7B) in all the shade treatments except one decreased outlier (40% light intensity at 45 d). (II) The stress responses also contain reactive oxygen species (ROS) and their scavenge systems. The ROS levels indicated by H_2O_2 (Fig. 7C) and $O_2^{\cdot-}$ (Fig. 7D) decreased when shade-treated compared to control excluding two increased cases (H_2O_2: 60% light intensity at 60 d; $O_2^{\cdot-}$: 10% light intensity at 45 d). The ROS scavenge enzyme activities in the shade treatments, such as POD (Fig. 7E), SOD (Fig. 7F),

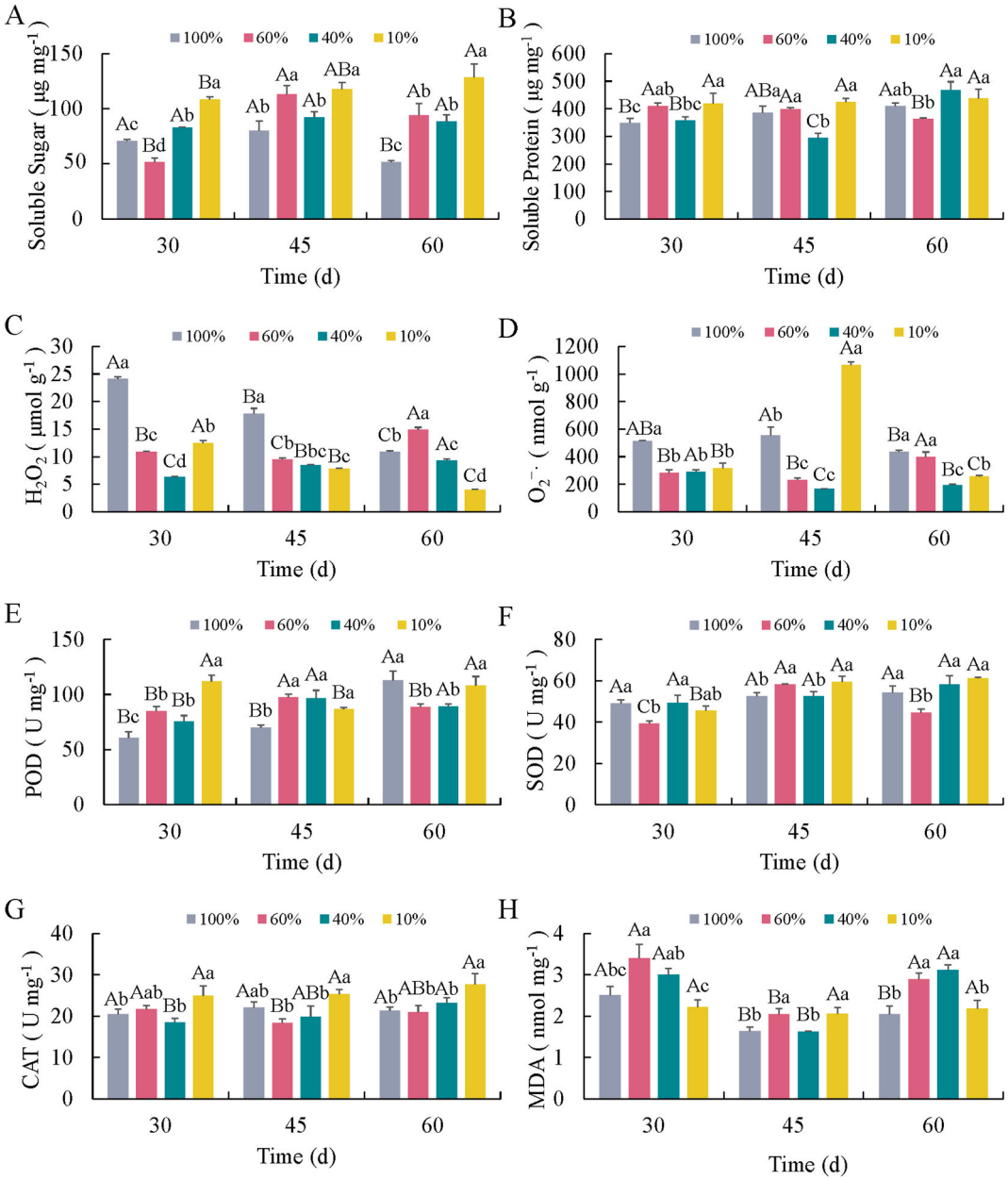

Fig. 7. Shade-induced stress physiological changes in *Spatholobus suberectus*. H_2O_2, hydrogen peroxide; $O_2^{\cdot-}$, superoxide anion radical; POD, peroxidase; SOD, superoxide dismutase; CAT, catalase; MDA, malonydialdehyde. Figure legends of shade treatments and statistical analyses are the same as in Fig. 3. (For interpretation of the references to colour in this figure legend, the reader is referred to the Web version of this article.)

CAT (Fig. 7G), were increased or at least comparable to those of the control, except for three deceased cases (POD: 60%- and 40%- light intensities at 60 d; SOD: 60% light intensity at 60 d). And the three antioxidant enzyme activities at 10% light intensity were much higher than or comparable to the other two intensities in all the shade treatments. (III) The ROS could attack cell membrane, induce lipid peroxidation, and generate MDA. The MDA contents are often used for membrane damage assessment. The MDA contents (Fig. 7H) in the shade treatments were all higher or comparable to control, especially at 60% light intensity in the three shade durations, indicating the adverse effects of low light. To sum up, these results suggested that although less ROS were produced at low light intensities, *S. suberectus* up-regulated related stress resistance factors to tolerate the low light stress.

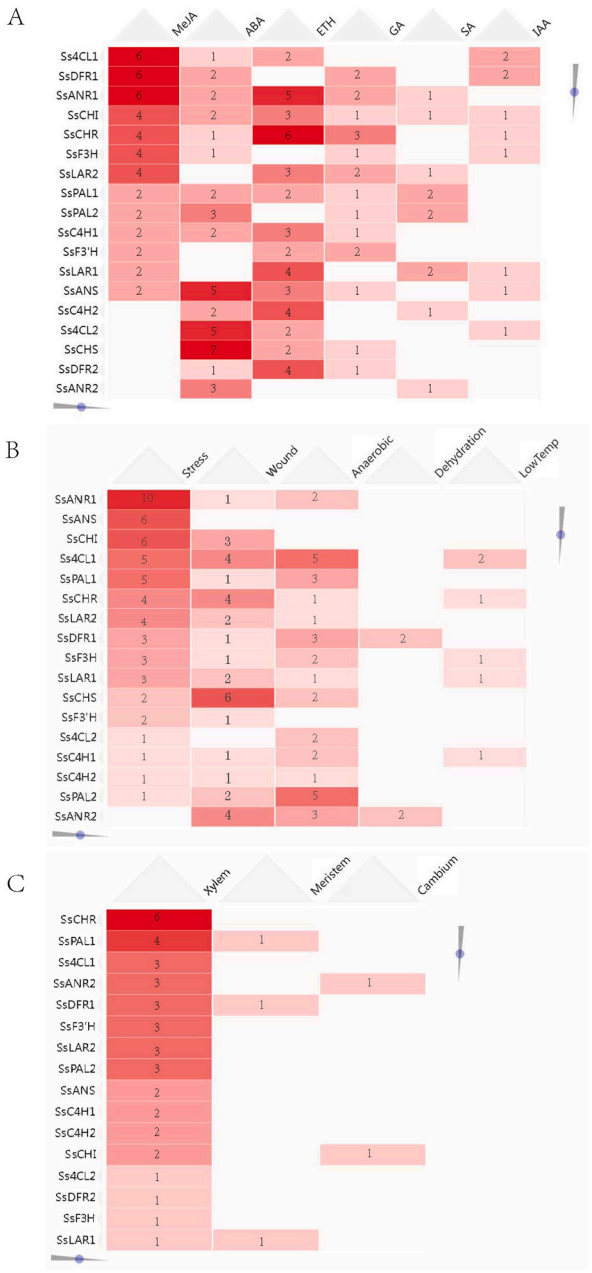

Fig. 8. Putative promoter *cis*-regulatory elements (CREs) of flavonoid biosynthetic genes in *Spatholobus suberectus*. (A) Phytohormone-related CREs (IAA-, GA-, MeJA-, ABA-, ETH-, and SA-responsive elements). IAA, auxin; GA, gibberellin; MeJA, methyl jasmonate; ABA, abscisic acid; ETH, ethylene; SA, salicylic acid. (B) Stress-related CREs (stress-, wound-, anaerobic-, dehydration- and low temperature-responsive elements). (C) Development-related CREs (meristem expression related elements, xylem-related elements, and development related elements). The row- and column-variables were ranked by variances. Numbers labelled are copy numbers of CREs.

3.6. Putative phytohormone-, stress- and development-related promoter cis-regulatory element analysis in S. suberectus

With reference to literatures describing CRE [18–20], the phytohormone-, stress-, and development-related CREs in 18 flavonoid biosynthetic pathway genes promoter regions were identified in *S. suberectus* and visualized by heatmap (Fig. 8).

First, the phytohormone-related CREs contained 6 types. Besides CREs related to our four examined phytohormones (IAA, GA, MeJA, and ABA), CREs related to ethylene (ETH) and salicylic acid (SA) were also detected (Fig. 8A). The phytohormone-related CREs and their motif sequences were as follows: (I) IAA-responsive element (TGA-element (AACGAC) and AuxRR-core sequence (GGTCCAT)); (II) GA-responsive element (P-box (CCTTTTG), CARE (CAACTCAC), and TATC-box (TATCCCA)); (III) MeJA-responsive element (CGTCA-motif (CGTCA) and TGACG-motif (TGACG)); (IV) ABA-responsive element (ACGT core sequence, such as ABRE (ACGTG), At˜ABRE (TACGTGTC), ABRE3a (TACGTG), and ABRE4 (CACGTA)); (V) ETH-responsive element (ERE (ATTTTAAA)); (VI) SA-responsive element (TCA-element (CCATCTTTTT) and TCA (TCATCTTCAT)). Each gene had at least two types of phytohormone-related CREs and only *SsCHI* had all the six types of phythormone CREs. According to their copy numbers, MeJA-responsive elements were the most abundant, and follows were ETH-, ABA-, GA-, SA-, and IAA-responsive elements.

Second, the stress-related CREs contained 5 types. They were present in 17 genes promoter regions except *SsDFR2* (Fig. 8B). The stress-related CREs and their motif sequences were as follows: (I) Stress-responsive element (defense and stress responsive element (TC-rich repeats (GTTTTCTTAC)) and stress responsive element (STRE (AGGGG and CCCCT))); (II) Wound-responsive element (WUN-motif (AAATTACT) and WRE3 (CCACCT)); (III) Anaerobic-responsive element (anaerobic induction (ARE (AAACCA)) and enhancer-like element involved in anoxic specific inducibility (GC-motif (CCCCCG)); (IV) Dehydration-responsive element (DRE (A/GCCGAC)); (V) Low-temperature-responsive element (LTR (CCGAAA)). The 17 genes had at least one types of stress-related CREs and at most four types of stress-related CREs. Copy numbers of the stress-responsive elements were the largest, and follows were wound-, anaerobic-, low temperature-, and dehydration-responsive elements.

Third, the development-related CREs contained 3 types. They were present in 16 genes promoter regions except *SsCHS* and *SsANR1* (Fig. 8C). The development-related CREs and their motif sequences were as follows: (I) Meristem expression related element (CAT-box (GCCACT)); (II) Xylem-related element (xylem-specific expression element (AC-I ((T/C)C(T/C)(C/T)ACC(T/C)ACC) and AC-II (TCACCAACCCCC)), secondary xylem development related element (AAGAA motif (GAAAGAA and gGTAAAGAAA)); (III) Vascular cambium development related element (HD-ZIP3 motif (GTAAT (G/C)ATTAC)). The meristem expression related elements were presented in *SsPAL1*, *SsDFR1*, and *SsLAR1*.The xylem-related elements were the most abundant and presented in all the 16 genes. The vascular cambium development related elements were presented in *SsCHI* and *SsANR2*.

Overall, the presence of interested CREs in *S. suberectus* revealed that the flavonoid pathway genes were potentially involved in hormonal induction, stress response, and plant development.

4. Discussion

4.1. S. suberectus exhibited broad resilience to light environmental change

In nature wild *S. suberectus* distributes in diverse habitats, implying it might come across and overcome a variety of environmental stresses in different niches. This strong survival capacity was also demonstrated in our study. The cultivated *S.suberectus* displayed great vitality when shaded, such as sustained plant growth development (Fig. 3), regulated plant hormone (Fig. 4), variated flavonoids contents (Fig. 5) and gene expression levels (Fig. 6), increased soluble sugar and promoted antioxidant stress resistance levels (Fig. 7).

However, two aspects should be noticed. First, the specific shade responses to each treatment were irregular and it was difficult to summarize a law of responses and specify which treatment was the best for *S. suberectus*' growth and development. Nonetheless, as to the plant growth morphological changes, it can be concluded that the 40% light intensity was more beneficial for the stem growth than 60%- and 10%- light intensities (Fig. 3). Second, the shading effects were strengthened over time. To be exact, even if there were profits at some short-term shade durations, it was likely to be diminished or reversed and became unfavorable at long-term shade durations. Taken the stem diameter as an example, it is one of the commercial standards for *Spatholobi caulis* in herbal medicine market, but the shade-induced stem diameter increases were gradually dwindled down when shade durations prolonged. For instance, the basal stem diameter increments at 40% light intensity were increased 1.1-fold at 30 d, but these increases were 97.9% at 45 d and 50.7% at 60 d. Similarly, the new stem diameter increments at 40% light intensity were increased 43.8% at 30 d, but these increases were 44.7% at 45 d and 20.7% at 60 d. Moreover, the flavonoids changes discussed below also demonstrated this shade duration time effect. Therefore, for better interests, the removal of shading is necessary in the end.

Nonetheless, the underlying mechanisms behind the shade-induced responses needed to be clarified and it would be discussed in the following paragraphs.

4.2. The integrated light and phytohormone signaling determined S. suberectus' shade responses

The shade-induced morphological (Fig. 3) and plant hormonal (Fig. 4) changes in *S. suberectus*, such as decreased basal- and new-stem diameter increments, increased new stem height increments, and unchanged leaf numbers, enhanced auxin/IAA and GA levels, were part of the shade avoidance syndrome. Normally the shade induced phenotypic plasticity includes elongated hypocotyl/stem/petiole, hyponastic petiole, inhibited leaf size, less branching, early flowering, etc [21]. A cascade involving photoreception, light signal transduction, and plant hormone integration explained the light-induced responses [22].

The E3 ubiquitin ligase CONSTITUTIVE PHOTOMORPHOGENIC 1 (COP1), and the basic leucine-zipper (bZIP) factor ELONGATED

HYPOCOTYL 5 (HY5), constitutes the COP1-HY5 module and centers in the cascade [23]. When shaded, the shade signals (low red/far-red light ratio, low blue/green light ratio, and low UV-B signal) are perceived by photoreceptors (PHYTOCHORMES (PHYs), CRYPTOCHROMES (CRYs), and UV RESISTANCE LOCUS 8 (UVR8)), COP1 rapidly re-accumulates in the nucleus, and COP1 activity increases and enhances HY5 degradation [24,25]. HY5 functions pivotally by regulating downstream light-responsive gene expressions positively or negatively, causing wide physiological and developmental responses [26].

Plant hormones interact with COP1 and HY5 and integrate into the light signaling network [27,28]. It was reported that under shade, auxin/IAA and GA were activated to promote stem elongation, MeJA was repressed to attenuate limited resources reallocating to defense, and ABA was increased to repress branching [22,29]. As to this study, the increases of IAA and GA after shading were pronounced, but the shade-induced decreases of MeJA and the increases of ABA were only shown in several cases (Fig. 4). This was attributed to the multi-roles, crosstalks and signalings of phytohormones, which were functioned in versatile aspects involving in plant growth, development, biotic and abiotic stress responses [30–32]. For example, MeJA not only induces defensive compounds against pathogens and abiotic stress, but also mitigates oxidative damage and interacts with other plant hormones [33,34]. Therefore the fact that MeJA contents at 10% light intensity were all higher than or at least equal to control seemed plausible. Likewise, ABA not only acts as branching inhibitor under shade, but also involves in stomatal closure, osmotic regulation, growth inhibition, pathogen response, and other adaptations to stress [35–37]. So the results that ABA contents detected were actually decreased in some shading cases were understandable. On the whole, shading effects and other complicated mechanisms determined the actual contents of IAA, GA, MeJA, and ABA detected in this study.

Taken together, the interwoven of light signaling with phytohormone signaling determined the shade-induced growth and development of *S. suberectus*.

4.3. The short-term shade improved S. suberectus' medicinal value

Shade treatments changed secondary metabolites in *S. suberectus*, especially flavonoids. Flavonoids function as photoreceptors, light screening, antioxidants, etc. [38,39], and these traits are helpful for plant to adapt to low light stress. But the roles of flavonoids as therapeutic agents make us focus more on their shade-induced content changes, which are closely related to the medicinal value of *S. suberectus* [40,41].

Our study demonstrated that short-term shading (30 d) improved the medicinal value of *S. suberectus*. This could be concluded from the three changed aspects at 30 d-shade durations (Fig. 5). First, contents of total flavonoids, which are the main bioactive components of *S. suberectus*, were significantly increased at 10% light intensity. Second, contents of gallated catechins, which have stronger pharmacological efficacy than non-gallated catechins, were significantly increased or comparable to those of the control at three shade light intensities. Third, contents of epigallocatechin gallate, which is the most potent beneficial catechin, were highest at 60% light intensity. To trace the reason, the increased bioactive components were attributed to the increased biosynthesis genes expressions at 30 d-shade durations (Fig. 6). Specifically, gene expressions of *SsPAL1, SsPAL2, SsC4H1, SsC4H2, Ss4CL1* and *Ss4CL2* at 40% light intensity, and *Ss4CL2* at 60%- light intensity, were increased in the phenylalanine—4-coumaroyl-CoA pathway; gene expressions of *SsCHS* and *SsCHI* at 10% light intensity were increased in the 4-coumaroyl-CoA—naringenin pathway; and gene expressions of *SsF3H*, *SsF3′H*, *SsDFR1*, *SsDFR2*, *SsLAR2*, *SsANS*, *SsANR1* and *SsANR2* at three shade light intensities, and *SsLAR1* expressions at 60%-light intensity, were increased in the dihydrokaempferol—dihydroquercetin pathway and dihydroflavonols—catechins pathway.

However, at 10% light intensity in the three shade durations (Fig. 5), the metabolites (total flavonoids, catechin gallate, epicatechin gallate, gallocatechin gallate, and epigallocatechin gallate) decreased over time indicated the normal flavonoid accumulation with plant development pattern was broken, suggesting the negative effects of very low light on *S. suberectus*' growth and development. Therefore, the tradeoff between medicinal value improvement and plant growth retardation needs to be concerned when considering the short-term shade-induced profits commercially.

Furthermore, our study also demonstrated the benefits from short-term shading (30 d) were unsustainable, as contents of total flavonoids and all eight catechins were decreased with increased shade duration time (45 d, 60 d) (Fig. 5). Similarly, this could be explained by their corresponding biosynthesizing gene expressions at 45 d- and 60 d-shade durations (Fig. 6). To be concise, the decreased gene expressions at both times were listed as follows: The gene expression decreases of *SsPAL1*, *SsPAL2*, *SsC4H1*, *SsC4H2*, and *Ss4CL1* in the phenylalanine—4-coumaroyl-CoA pathway; the decreases of *SsCHS* in the 4-coumaroyl-CoA—naringenin pathway; and the decreases of *SsF3H*, *SsF3′H*, *SsDFR1*, *SsDFR2*, *SsLAR2*, *SsANS*, *SsANR1* and *SsANR2* in the dihydrokaempferol—dihydroquercetin pathway and dihydroflavonols—catechins pathway.

An exceptional case was isoliquiritigenin, whose contents were unaffected in all the shade treatments (Fig. 5). Previous study explained that the reason why isoliquiritigenin contents were less affected by its upper flavonoid biosynthetic genes because it was an intermediate metabolite in the pathway [4]. But here we thought the direct reason was that the gene expressions of *SsCHR* in the isoliquiritigenin biosynthesizing pathway were unchanged in the shade treatments (Fig. 6).

All in all, the shade in short-term improved while in long-term depreciated the medicinal value of *S. suberectus*, and this was attributed to the flavonoid biosynthesizing gene expressions variations under shade.

4.4. The high antioxidant capacity enhanced S. suberectus' shade tolerance

The stress physiological parameters measured in this study, such as increased soluble sugar, merely unchanged soluble protein, decreased ROS levels, increased MDA, and increased ROS scavenge levels (Fig. 7), reflected the adaptive strategies taken by *S. suberectus* in the shade treatments.

Soluble sugar is the product of photosynthesis and mainly includes sucrose, glucose, and fructose. It serves as energy source, nutrient, osmoprotectant, and ROS scavengers for plant growth and stress tolerance [42]. Theoretically the content of soluble sugar would decrease when photosynthesis is inhibited by shading. While in this study, the soluble sugar content was increased after shading, demonstrating the shade tolerance of *S. suberectus*.

The increased ROS scavenge enzyme activities (POD, SOD, and CAT) also indicated the higher antioxidant capacity of *S. suberectus*. For example, the three enzymes activities at three shade durations were all increased at 10% light intensity, demonstrating the well ROS clearance capacity of *S. suberectus* in low light stress.

Therefore, in this study, although there were shade-induced damages on biomembrane as indicated by MDA contents, the oxidative levels of *S. suberectus* were low as indicated by H_2O_2 and $O_2^{\cdot-}$ levels.

In a few words, the higher antioxidant levels of *S. suberectus* further demonstrated its well survival capacity under shade.

4.5. The putative cis-regulatory element endowed S. suberectus with potential stress tolerance

In this study, a number of phytohormone-related CREs (IAA-, GA-, MeJA-, ABA-, ETH-, and SA-responsive elements), stress-related CREs (stress-, wound-, anaerobic-, dehydration- and low temperature-responsive elements), and development-related CREs (meristem expression related elements, xylem-related elements, and vascular cambium development related elements) were identified in *S. suberectus*' flavonoid biosynthetic genes' promoter regions (Fig. 8).

On one hand, this result indicated that the pathway genes could be induced or stimulated either by six types of plant hormones or by multiple biotic/abiotic stresses, implying the involvement of phytohormone and stress-resistant factors when *S. suberectus* confronted with stress. For instance, the involvement of MeJA, ETH, and SA, the well-known plant hormones participating in biotic and abiotic stresses [43], helped *S. suberectus* to become shade tolerant.

On the other hand, this result indicated that these pathway genes could also exert influences on plant development, especially xylem-related. Two xylem-related CREs were identified in this study. To be specific, the *cis*-element AC-I/AC-II relates to lignin biosynthesis and the *cis*-element AAGAA motif relates to secondary xylem development. Lignin biosynthesis functions in plant growth, development, lodging resistance, and stress responses [44]. Secondary xylem comprises the bulk of stems and roots, transporting water and minerals and providing supporting functions for plant survival [45]. For an herbal medicine using stem as medicinal part, the presences of xylem-related CREs were important for *S. suberectus*' medicinal value as well as its stress tolerance.

Moreover, MeJA-responsive element, stress-responsive element, and xylem-related elements were the most plentiful CREs relating to phytohormone, stress, and development respectively. And these copy number variations of CREs indicated their differences in responses to various stimulations [7].

Collectively, the variety of CREs present in flavonoid biosynthetic genes gave *S. suberectus* the benefits of stress tolerance.

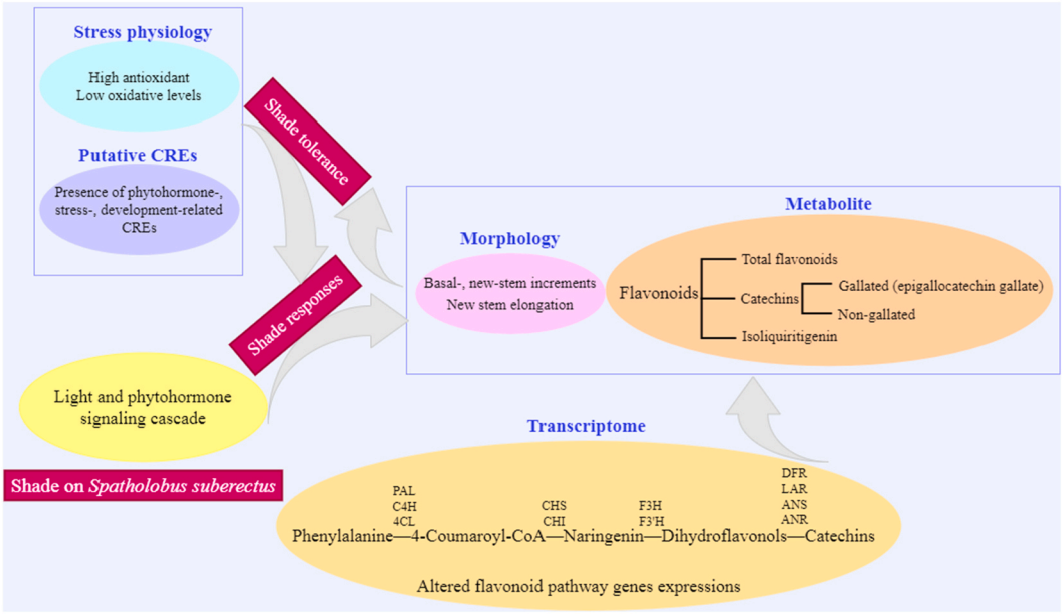

Fig. 9. Proposed model of *Spatholobus suberectus*' shade response and shade tolerance. When shaded, the light and phytohormone signaling cascade determined *S. suberectus*' shade responses, resulting in morphological and metabolic changes. The latter changes were attributed to the flavonoid pathway gene expression alterations. Shade also led to high antioxidant and low oxidative levels in *S. suberectus*. These variations together with the presence of important promoter *cis*-regulatory elements (CREs) enabled *S. suberectus*' to be shade tolerant. Abbreviations of enzymes are the same as in Fig. 1. (For interpretation of the references to colour in this figure legend, the reader is referred to the Web version of this article.)

4.6. Proposed model of *S. suberectus*' shade response and shade tolerance

In summary, a model was proposed to illustrate *S. suberectus*' shade response and shade tolerance (Fig. 9). Photoreceptors sensed shade signals and the light signal transduction integrated with phytohormones decided *S. suberectus*' shade responses. Shade resulted in variations of stem morphology, flavonoid contents, flavonoid pathway gene expressions, and antioxidant levels. These response changes combined with the presence of some important CREs helped *S. suberectus* to become shade tolerant.

5. Conclusions

In conclusion, *S. suberectus* showed broad-resilience to shade stress. Regarding to morphological factors, 40% light intensity was more beneficial for the stem growth of *S. suberectus*. Plant hormones were involved in the regulation of shade-induced responses. Shade in short-term improved while in long-term depreciated the medicinal value of *S. suberectus*, which was attributed to the flavonoid biosynthesizing gene expressions variations under shade. The high antioxidant capacity and low oxidative levels enabled the shade resistance. The presence of phytohormone-, stress-, and development-related CREs in flavonoid biosynthetic genes elucidates the basis of *S. suberectu*'s stress tolerance.

Data availability statement

Data will be made available on request.

CRediT authorship contribution statement

Shuangshuang Qin: Writing – review & editing, Writing – original draft, Funding acquisition, Formal analysis, Conceptualization. **Ying Liang:** Project administration, Methodology, Investigation. **Guili Wei:** Project administration, Methodology, Investigation. **Fan Wei:** Validation, Resources, Data curation. **Kunhua Wei:** Validation, Resources, Data curation. **Xiaoying Chen:** Writing – review & editing, Writing – original draft, Funding acquisition, Formal analysis, Conceptualization.

Declaration of competing interest

The authors declare that they have no known competing financial interests or personal relationships that could have appeared to influence the work reported in this paper.

Acknowledgments

This work was supported by National Natural Science Foundation of China (grant number 82160723), Natural Science Foundation of Guangxi Zhuang Autonomous Region (grant number 2021GXNSFAA196054), and Independent Subject of Guangxi Key Laboratory of Medicinal Resources Protection and Genetic Improvement (grant number KL2022ZZ03).

Appendix A. Supplementary data

Supplementary data to this article can be found online at https://doi.org/10.1016/j.heliyon.2024.e28077.

References

[1] Y. Liu, Q. Xiang, Q. Liang, J. Shi, J. He, Genus *Spatholobus*: a comprehensive review on ethnopharmacology, phytochemistry, pharmacology, and toxicology, Food Funct. 13 (2022) 7448–7472, https://doi.org/10.1039/D2FO00895E.
[2] Y. Pan, X. Luo, P. Gong, *Spatholobi caulis*: a systematic review of its traditional uses, chemical constituents, biological activities and clinical applications, J. Ethnopharmacol. 317 (2023) 116854, https://doi.org/10.1016/j.jep.2023.116854.
[3] F. Zhang, K. Ganesan, Q. Liu, J. Chen, A review of the pharmacological potential of *Spatholobus suberectus* Dunn on cancer, Cells 11 (2022) 2885, https://doi.org/10.3390/cells11182885.
[4] S. Qin, K. Wei, Z. Cui, Y. Liang, M. Li, L. Gu, C. Yang, X. Zhou, L. Li, W. Xu, C. Liu, J. Miao, Z. Zhang, Comparative genomics of *Spatholobus suberectus* and insight into flavonoid biosynthesis, Front. Plant Sci. 11 (2020) 528108, https://doi.org/10.3389/fpls.2020.528108.
[5] S. Qin, L. Wu, K. Wei, Y. Liang, Z. Song, X. Zhou, S. Wang, M. Li, Q. Wu, K. Zhang, Y. Hui, S. Wang, J. Miao, Z. Zhang, A draft genome for *Spatholobus suberectus*, Sci. Data 6 (2019) 113, https://doi.org/10.1038/s41597-019-0110-x.
[6] Y. Cui, Q. Cao, Y. Li, M. He, X. Liu, Advances in *cis*-element- and natural variation-mediated transcriptional regulation and applications in gene editing of major crops, J. Exp. Bot. 74 (2023) 5441–5457, https://doi.org/10.1093/jxb/erad248.
[7] C. Zou, K. Sun, J.D. Mackaluso, A.E. Seddon, R. Jin, M.F. Thomashow, S.-H. Shiu, *Cis*-regulatory code of stress-responsive transcription in *Arabidopsis thaliana*, Proc. Natl. Acad. Sci. U.S.A. 108 (2011) 14992–14997, https://doi.org/10.1073/pnas.1103202108.
[8] F.F. Mohd Yusof, J.S. Yaacob, N. Osman, M.H. Ibrahim, W.A.A.Q.I. Wan-Mohtar, Z. Berahim, N.A. Mohd Zain, Shading effects on leaf gas exchange, leaf pigments and secondary metabolites of *polygonum minus* Huds., an aromatic medicinal herb, Plants 10 (2021) 608, https://doi.org/10.3390/plants10030608.
[9] Y. Shan, C. Deng, W. Hu, J. Chen, X. Chen, Q. Qin, S. Zheng, Long-term, high-intensity shading enhances triterpene production of loquat leaf through increasing foliar mineral nutrients, Sci. Hortic 260 (2020) 108873, https://doi.org/10.1016/j.scienta.2019.108873.

[10] N. Tmušić, Z.S. Ilić, L. Milenković, L. Šunić, D. Lalević, Ž. Kevrešan, J. Mastilović, L. Stanojević, D. Cvetković, Shading of medical plants affects the phytochemical quality of herbal extracts, Horticulturae 7 (2021) 437, https://doi.org/10.3390/horticulturae7110437.
[11] P. Zubay, K. Ruttner, M. Ladányi, J. Deli, É. Németh Zámboriné, K. Szabó, In the shade – screening of medicinal and aromatic plants for temperate zone agroforestry cultivation, Ind. Crops Prod. 170 (2021) 113764, https://doi.org/10.1016/j.indcrop.2021.113764.
[12] L. Milenković, Z.S. Ilić, L. Šunić, N. Tmušić, L. Stanojević, J. Stanojević, D. Cvetković, Modification of light intensity influence essential oils content, composition and antioxidant activity of thyme, marjoram and oregano, Saudi J. Biol. Sci. 28 (2021) 6532–6543, https://doi.org/10.1016/j.sjbs.2021.07.018.
[13] Y.-X. Ma, C. Sutcharitchan, X.-D. Li, Q. Meng, X. Wang, S. Ji, Y.-J. Cui, Combined application of extended depth of field imaging, image stitching and polarized microscopy techniques in identification of *Spatholobus suberectus*, Chinese Herb. Med. 12 (2020) 367–374, https://doi.org/10.1016/j.chmed.2020.10.001.
[14] B. Li, C.N. Dewey, RSEM: accurate transcript quantification from RNA-Seq data with or without a reference genome, BMC Bioinform 12 (2011) 323, https://doi.org/10.1186/1471-2105-12-323.
[15] M. Lescot, P. Déhais, G. Thijs, K. Marchal, Y. Moreau, Y. Van de Peer, P. Rouzé, S. Rombauts, PlantCARE, a database of plant *cis*-acting regulatory elements and a portal to tools for *in silico* analysis of promoter sequences, Nucleic Acids Res. 30 (2002) 325–327, https://doi.org/10.1093/nar/30.1.325.
[16] K. Higo, Y. Ugawa, M. Iwamoto, T. Korenaga, Plant cis-acting regulatory DNA elements (PLACE) database: 1999, Nucleic Acids Res. 27 (1999) 297–300, https://doi.org/10.1093/nar/27.1.297.
[17] N.F. Fernandez, G.W. Gundersen, A. Rahman, M.L. Grimes, K. Rikova, P. Hornbeck, A. Ma'ayan, Clustergrammer, a web-based heatmap visualization and analysis tool for high-dimensional biological data, Sci. Data 4 (2017) 170151, https://doi.org/10.1038/sdata.2017.151.
[18] Q.-u. ain-Ali, N. Mushtaq, R. Amir, A. Gul, M. Tahir, F. Munir, Genome-wide promoter analysis, homology modeling and protein interaction network of Dehydration Responsive Element Binding (DREB) gene family in *Solanum tuberosum*, PLoS One 16 (2021) e0261215, https://doi.org/10.1371/journal.pone.0261215.
[19] H. Maqsood, F. Munir, R. Amir, A. Gul, Genome-wide identification, comprehensive characterization of transcription factors, cis-regulatory elements, protein homology, and protein interaction network of DREB gene family in *Solanum lycopersicum*, Front. Plant Sci. 13 (2022) 1031679, https://doi.org/10.3389/fpls.2022.1031679.
[20] C.N. Tang, W. Wan Abdullah, C.Y. Wee, Z.N. Balia Yusof, W.S. Yap, W.H. Cheng, N.A. Baharum, J. Ong-Abdullah, J.Y. Loh, K.S. Lai, Promoter cis-element analyses reveal the function of αVPE in drought stress response of *Arabidopsis*, Biology 12 (2023) 430, https://doi.org/10.3390/biology12030430.
[21] Y. Wu, W. Gong, W. Yang, Shade inhibits leaf size by controlling cell proliferation and enlargement in soybean, Sci. Rep. 7 (2017) 9259, https://doi.org/10.1038/s41598-017-10026-5.
[22] Y. Liu, F. Jafari, H. Wang, Integration of light and hormone signaling pathways in the regulation of plant shade avoidance syndrome, aBIOTECH 2 (2021) 131–145, https://doi.org/10.1007/s42994-021-00038-1.
[23] A. Bhatnagar, S. Singh, J.P. Khurana, N. Burman, HY5-COP1: the central module of light signaling pathway, J. Plant Biochem. Biotechnol. 29 (2020) 590–610, https://doi.org/10.1007/s13562-020-00623-3.
[24] M. Pacín, M. Legris, J.J. Casal, COP1 re-accumulates in the nucleus under shade, Plant J. 75 (2013) 631–641, https://doi.org/10.1111/tpj.12226.
[25] A. Sharma, B. Sharma, S. Hayes, K. Kerner, U. Hoecker, G.I. Jenkins, K.A. Franklin, UVR8 disrupts stabilisation of PIF5 by COP1 to inhibit plant stem elongation in sunlight, Nat. Commun. 10 (2019) 4417, https://doi.org/10.1038/s41467-019-12369-1.
[26] Y. Xiao, L. Chu, Y. Zhang, Y. Bian, J. Xiao, D. Xu, HY5: a pivotal regulator of light-dependent development in higher plants, Front. Plant Sci. 12 (2022) 800989, https://doi.org/10.3389/fpls.2021.800989.
[27] S.N. Gangappa, J.F. Botto, The multifaceted roles of HY5 in plant growth and development, Mol. Plant 9 (2016) 1353–1365, https://doi.org/10.1016/j.molp.2016.07.002.
[28] X. Xie, H. Cheng, C. Hou, M. Ren, Integration of light and auxin signaling in shade plants: from mechanisms to opportunities in urban agriculture, Int. J. Mol. Sci. 23 (2022), https://doi.org/10.3390/ijms23073422.
[29] C. Yang, L. Li, Hormonal regulation in shade avoidance, Front. Plant Sci. 8 (2017) 1527, https://doi.org/10.3389/fpls.2017.01527.
[30] D. Egamberdieva, S.J. Wirth, A.A. Alqarawi, E.F. AbdAllah, A. Hashem, Phytohormones and beneficial microbes: essential components for plants to balance stress and fitness, Front. Microbiol. 8 (2017) 2104, https://doi.org/10.3389/fmicb.2017.02104.
[31] A. Mukherjee, A.K. Gaurav, S. Singh, S. Yadav, S. Bhowmick, S. Abeysinghe, J.P. Verma, The bioactive potential of phytohormones: a review, Biotechnol. Rep. 35 (2022) e00748, https://doi.org/10.1016/j.btre.2022.e00748.
[32] B. Zhao, Q. Liu, B. Wang, F. Yuan, Roles of phytohormones and their signaling pathways in leaf development and stress responses, J. Agric. Food Chem. 69 (2021) 3566–3584, https://doi.org/10.1021/acs.jafc.0c07908.
[33] Y. Wang, S. Mostafa, W. Zeng, B. Jin, Function and mechanism of jasmonic acid in plant responses to abiotic and biotic stresses, Int. J. Mol. Sci. 22 (2021) 8568, https://doi.org/10.3390/ijms22168568.
[34] X. Yu, W. Zhang, Y. Zhang, X. Zhang, D. Lang, X. Zhang, The roles of methyl jasmonate to stress in plants, Funct. Plant Biol. 46 (2019) 197–212, https://doi.org/10.1071/FP18106.
[35] B.P. Brookbank, J. Patel, S. Gazzarrini, E. Nambara, Role of basal ABA in plant growth and development, Genes 12 (2021) 1936, https://doi.org/10.3390/genes12121936.
[36] K. Chen, G.J. Li, R.A. Bressan, C.P. Song, J.K. Zhu, Y. Zhao, Abscisic acid dynamics, signaling, and functions in plants, J. Integr. Plant Biol. 62 (2020) 25–54, https://doi.org/10.1111/jipb.12899.
[37] T. Yoshida, A. Christmann, K. Yamaguchi-Shinozaki, E. Grill, A.R. Fernie, Revisiting the basal role of ABA – roles outside of stress, Trends Plant Sci. 24 (2019) 625–635, https://doi.org/10.1016/j.tplants.2019.04.008.
[38] P.G. Pietta, Flavonoids as antioxidants, J. Nat. Prod. 63 (2000) 1035–1042, https://doi.org/10.1021/np9904509.
[39] A. Shomali, S. Das, N. Arif, M. Sarraf, N. Zahra, V. Yadav, S. Aliniaeifard, D.K. Chauhan, M. Hasanuzzaman, Diverse physiological roles of flavonoids in plant environmental stress responses and tolerance, Plants 11 (2022) 3158, https://doi.org/10.3390/plants11223158.
[40] M.C. Dias, D. Pinto, A.M.S. Silva, Plant flavonoids: chemical characteristics and biological activity, Molecules 26 (2021) 5377, https://doi.org/10.3390/molecules26175377.
[41] A. Ullah, S. Munir, S.L. Badshah, N. Khan, L. Ghani, B.G. Poulson, A.H. Emwas, M. Jaremko, Important flavonoids and their role as a therapeutic agent, Molecules 25 (2020) 5243, https://doi.org/10.3390/molecules25225243.
[42] S. Afzal, N. Chaudhary, N.K. Singh, Role of soluble sugars in metabolism and sensing under abiotic stress, in: T. Aftab, K.R. Hakeem (Eds.), Plant Growth Regulators: Signalling under Stress Conditions, Springer International Publishing, Cham, 2021, pp. 305–334.
[43] N. Li, X. Han, D. Feng, D. Yuan, L.J. Huang, Signaling crosstalk between salicylic acid and ethylene/jasmonate in plant defense: Do we understand what they are whispering? Int. J. Mol. Sci. 20 (2019) 671, https://doi.org/10.3390/ijms20030671.
[44] Q. Liu, L. Luo, L. Zheng, Lignins: biosynthesis and biological functions in plants, Int. J. Mol. Sci. 19 (2018) 335, https://doi.org/10.3390/ijms19020335.
[45] P. Sun, H. Wang, P. Zhao, Q. Yu, Y. He, W. Deng, H. Guo, The regulation of xylem development by transcription factors and their upstream microRNAs, Int. J. Mol. Sci. 23 (2022) 10134, https://doi.org/10.3390/ijms231710134.